

Reduction of Pesticide Toxicity Under Field-Relevant Conditions? The Interaction of Titanium Dioxide Nanoparticles, Ultraviolet, and Natural Organic Matter

Simon Lüderwald,^a Frederik Meyer,^a Verena Gerstle,^a Lisa Friedrichs,^a Katrin Roling,^a Verena C. Schreiner,^a Nikita Bakanov,^a Ralf Schulz,^{a,b} and Mirco Bundschuh^{a,c,*}

^aIES Landau, Institute for Environmental Sciences, University of Koblenz-Landau, Landau, Germany

^bEusserthal Ecosystem Research Station, University of Koblenz-Landau, Eusserthal, Germany

^cDepartment of Aquatic Sciences and Assessment, Swedish University of Agricultural Sciences, Uppsala, Sweden

Abstract: In surface waters, the illumination of photoactive engineered nanomaterials (ENMs) with ultraviolet (UV) light triggers the formation of reactive intermediates, consequently altering the ecotoxicological potential of co-occurring organic micropollutants including pesticides due to catalytic degradation. Simultaneously, omnipresent natural organic matter (NOM) adsorbs onto ENM surfaces, altering the ENM surface properties. Also, NOM absorbs light, reducing the photo(cata)lytic transformation of pesticides. Interactions between these environmental factors impact 1) directly the ecotoxicity of photoactive ENMs, and 2) indirectly the degradation of pesticides. We assessed the impact of field-relevant UV radiation (up to 2.6 W UVA/m²), NOM (4 mg TOC/L), and photoactive ENM (nTiO₂, 50 µg/L) on the acute toxicity of 6 pesticides in *Daphnia magna*. We selected azoxystrobin, dimethoate, malathion, parathion, permethrin, and pirimicarb because of their varying photo- and hydrolytic stabilities. Increasing UVA alone partially reduced pesticide toxicity, seemingly due to enhanced degradation. Even at 50 µg/L, nano-sized titanium dioxide (nTiO₂) reduced but also increased pesticide toxicity (depending on the applied pesticide), which is attributable to 1) more efficient degradation and potentially 2) photocatalytically induced formation of toxic by-products. Natural organic matter 1) partially reduced pesticide toxicity, not evidently accompanied by enhanced pesticide degradation, but also 2) inhibited pesticide degradation, effectively increasing the pesticide toxicity. Predicting the ecotoxicological potential of pesticides based on their interaction with UV light or interaction with NOM was hardly possible, which was even more difficult in the presence of nTiO₂. *Environ Toxicol Chem* 2020;39:2237–2246. © 2020 The Authors. *Environmental Toxicology and Chemistry* published by Wiley Periodicals LLC on behalf of SETAC.

Keywords: Photolysis; Photocatalysis; Titanium dioxide; Pesticide; UV radiation; Natural organic matter

INTRODUCTION

In recent years, the application of engineered nanomaterials (ENMs) has increased rapidly (Keller and Lazareva 2014). Consequently, ENMs are likely to enter the aquatic environment, mainly through runoff from agricultural fields treated with sewage sludge as fertilizer or the release of wastewater (Gottschalk and Nowack 2011; Westerhoff et al. 2011). Once

entering surface waters, the fate of ENMs is influenced by a multitude of environmental factors. Irradiation with ultraviolet (UV) light is a factor which is of particular concern for photocatalytically active metal oxides such as nano-sized titanium dioxide (nTiO₂) or zinc oxide (Valenzuela et al. 2002; Ouyang et al. 2019). Under these conditions, the formation of reactive oxygen species (ROS) is triggered (Ma et al. 2012). This formation of ROS can also support water treatment (Thiruvengkatachari et al. 2008) by reducing the ecotoxicological potential of co-occurring organic micropollutants including pesticides (Hariharan 2006; Bundschuh et al. 2011; Seitz et al. 2012). In addition to UV, natural organic matter (NOM) is known for its potential to alter the surface properties of ENMs by adsorption (Aiken et al. 2011). Moreover, NOM adsorbs light, affecting the photo(cata)lytic transformation of organic micropollutants (Garg et al. 2011). The interaction with these

This article includes online-only Supplemental Data.

This is an open access article under the terms of the Creative Commons Attribution-NonCommercial License, which permits use, distribution and reproduction in any medium, provided the original work is properly cited and is not used for commercial purposes.

* Address correspondence to bundschuh@uni-landau.de

Published online 17 August 2020 in Wiley Online Library (wileyonlinelibrary.com).

DOI: 10.1002/etc.4851

environmental factors has significant influences on the ecotoxicological potential of photoactive ENMs (Bar-Ilan et al. 2013; Lüderwald et al. 2019) and indirectly affects the degradation of organic micropollutants (Thiruvengatachari et al. 2008; Seitz et al. 2012). It remains, however, unclear whether similar effects can be observed at field-relevant levels of ENMs, UV, and NOM.

Consequently, the present study aimed at addressing the presence of comparably low UV radiation (up to 2.6 W UVA/m²) recorded during a summer afternoon in the shade (Häder et al. 2007; Amiano et al. 2012), a field-relevant NOM (4 mg TOC/L, seaweed extract [Ryan et al. 2009]), and photoactive ENM concentration (nTiO₂, P25, 50 µg/L) on the acute toxicity of 6 pesticides toward the model organism *Daphnia magna*. We selected nTiO₂ because it is one of the most frequently applied ENMs, being used in personal care products, coatings, paints, and pigments (Piccinno et al. 2012; Keller and Lazareva 2014). Moreover, its predicted environmental concentration is in the micrograms per liter range (Gottschalk et al. 2013; Peters et al. 2018) and thus of the same order of magnitude as the concentration tested in the present study (Gondikas et al. 2014). As pesticides, we selected azoxystrobin, dimethoate, malathion, parathion, permethrin, and pirimicarb because of their varying photolytic (p-), and hydrolytic (h-) 50% degradation times (DT50s) and organic carbon–water partitioning coefficient (*K*_{OC}; Table 1). Pesticide concentrations were quantified for each exposure scenario (except for parathion and permethrin) right after the application (0 h), as well as after the termination of the experiment (96 h), allowing us to unveil the degradation efficacy, the resulting ecotoxicological potential, and the influence of UV radiation, nTiO₂, and NOM on this process.

We hypothesized that increasing UV radiation leads to reduced acute toxicity, which is explained by enhanced degradation of pesticides. Moreover, we expected this effect to be even more pronounced in the presence of nTiO₂ and/or NOM as a result of amplified pesticide degradation. Finally, we anticipated this impact to be of varying magnitude for the different pesticides, depending on their physicochemical properties. More specifically, the pesticides with a comparably low p-DT50 might undergo UV-induced detoxification, whereas for the pesticides with low susceptibility toward photolytic degradation the presence of nTiO₂ and NOM will induce their detoxification as a result of photocatalytic degradation.

MATERIALS AND METHODS

Nanoparticle characterization

The nTiO₂ we used was acquired as a powder (AEROXIDE® TiO₂ P25; Anatase-Rutile ratio ~75:25; Evonik) with an advertised primary particle size of 21 nm and a surface area of 50 ± 15 m²/g (Brunauer-Emmett-Teller). At the Institute for Particle Technology (TU Braunschweig, Braunschweig, Germany) an additive-free dispersion (80 g nTiO₂/L) was prepared by stirred media milling (PML 2; Bühler) using deionized water as a dispersant. Then, this dispersion was diluted with deionized water (stock dispersion, 2 g nTiO₂/L, nominal

TABLE 1: Pesticides, product and supplier information, along with the applied concentration ranges, photolytic and hydrolytic 50% degradation time (p- and h-DT50), and organic carbon–water partition coefficient (*K*_{OC}) of the pesticides used in the present study^a

Pesticide	Applied product	Supplier	Nominal concentrations (µg/L)	p-DT50 (days) at 20° C	h-DT50 (days) at 20° C	<i>K</i> _{OC}
Azoxystrobin	Ortiva®	Syngenta Agro	28.4, 56.8, 113.6, 227.2, 454.5, 909.1	8.7	Stable	589
Dimethoate	Perfekthion®	BASF SE	50, 100, 20, 400, 800, 1600, 3200	175	68	5–50
Malathion	PESTANAL®, analytical standard	Sigma-Aldrich	0.1, 0.2, 0.4, 0.8, 1.25, 2.5, 5	98	6.2	1800
Parathion	PESTANAL®, analytical standard	Sigma-Aldrich	0.3, 0.6, 1.25, 2.5, 5, 10	30	260	7660
Permethrin	PESTANAL®, analytical standard	Sigma-Aldrich	0.09, 0.18, 0.4, 0.7, 1.4, 2.8, 5.6	1	31	100 000
Pirimicarb	Pirimol®	Syngenta Agro	5, 10, 20, 40, 60, 80	0.5–6	Stable	56–800

^aDT50 and *K*_{OC} values are based on the active ingredient of the respective pesticide and were obtained from the Pesticides Properties Database (Lewis et al. 2016) and PubChem (National Center for Biotechnology Information 2019a, 2019b).

TABLE 2: Particle size (PS) distribution of the applied nTiO₂, i.e. intensity weighted average diameter, polydispersity index, as well as the 10th, 50th, and 90th percentiles, measured in the stock dispersion (0 h) and media (0, 24, 48, 72, and 96 h)^a

	Time (h)	Average diameter (nm)	PI	D10% (nm)	D50% (nm)	D90% (nm)
Stock	0	84	0.18	48	88	160
ASTM + nTiO ₂	0	417	0.21	92	241	709
	24	960	0.42	132	319	11 716
	48	1482	0.60	167	841	17 991
	72	2513	0.94	220	2239	58 881
	96	2535	0.95	255	20 951	50 057
ASTM + nTiO ₂ + NOM	0	376	0.24	87	256	918
	24	642	0.30	94	184	5618
	48	630	0.28	93	260	1622
	72	640	0.30	87	209	3484
	96	623	0.29	83	220	1534

^aFor PS behavior in the test medium under similar conditions, see Lüderwald (2019).

NOM = natural organic matter; nTiO₂ = nano-sized titanium dioxide; PI = polydispersity index.

concentration) and pH-stabilized (~3.25) by applying 120 µL of 2 M HCl/L. The intensity-weighted average hydrodynamic diameter of the stock dispersion was approximately 80 nm, measured via dynamic light scattering (DelsaNano C; Beckman Coulter) applying the following conditions: $n = 3$, 60 measurements each; temperature = 20 °C (Table 2). Before the application, the stock dispersion was sonicated for 10 min with a nominal power of 215 W and a sonication frequency of 35 Hz (SONOREX DIGITEC DT 514 H; Bandelin) as a standardized procedure to ensure a homogeneous particle distribution. Because inductively coupled plasma mass spectrometry (detailed in Rosenfeldt et al. 2014) indicated low differences (<20%) between measured and nominal concentrations of the product, the present study was based on the nominal nTiO₂ concentration (per Seitz et al. 2015). Transmission electron microscopic images of the ENM can be found in Supplemental Data, Figure S1.

Pesticides

The pesticides applied in the present study were purchased as either commercially available products (for azoxystrobin, dimethoate, and pirimicarb) or analytical standards (for malathion, parathion, and permethrin) and diluted in the respective test medium to achieve the desired nominal concentrations of the active ingredient (Table 1). Their selection is motivated by varying degrees of p- and h-DT50, ranging from 0.5 to 175 p-DT50 (days) and from 6.2 to 260 or stable h-DT50 (days; Table 1). Thereby, varying degrees in p- and h-DT50 will determine the rate of photolytic, photocatalytic, and hydrolytic degradation and therefore the potential of degradation and detoxification toward *D. magna*. Moreover, the pesticides were characterized by a high variation in their K_{OC} , ranging from 5 to 100 000 (Table 1). This broad range of adsorption capacity could influence the pesticides' interaction with NOM, which is likely to have an impact on their ecotoxicological potential.

Test organism

Daphnia magna (obtained from Eurofins-GAB) were kept in mass culture inside a climate-controlled chamber (Weiss Environmental Technology) at 20 ± 1 °C applying a 16:8-h light:dark photoperiod (fluorescent tubes; Osram L 58 W/840 lumilux cool white; visible light intensity 3.14 W/m²; UVA 0.01 W/m²; UVB 0.01 W/m²). Thereby, groups of 25 adult females were kept in 1.5 L of reconstituted hard freshwater, according to the ASTM International Standard Guide E729 (ASTM International 2007), which was, in addition, enriched with selenium, vitamins (thiamine hydrochloride, cyanocobalamin, and biotin), and seaweed extract (8 mg TOC/L; Marinure[®]). A renewal of the medium was carried out 3 times a week, and the organisms were daily fed on the green alga *Desmodesmus* sp. (corresponding to 200 µg C/organism/d).

Bioassay setup

For each pesticide, 4 individual exposure scenarios were realized, which in the following sections are referred to as test series: 1) pesticide exposure only (PEST), 2) pesticide exposure in the presence of 50 µg/L nTiO₂ (PEST + nTiO₂), 3) pesticide exposure in the presence of 4 mg TOC/L (PEST + NOM), and 4) combination of pesticide exposure in the presence of 50 µg/L nTiO₂ and 4 mg TOC/L (PEST + nTiO₂ + NOM). Each test series covered 4 levels with increasing UVA radiation, applying comparatively low but environmentally relevant levels (0–2.6 W UVA/m², UVA I–UVA IV; Table 3; Häder et al. 2007). The different UVA levels of radiation were achieved by attaching UV-porous curtains of varying efficiency to the UV tubes (per Lüderwald et al. 2019).

The tests were based on test guideline 202 (Organisation for Economic Co-operation and Development 2004), with the following 2 adaptations: 1) the test duration was prolonged to 96 h, as recommended for testing with nanomaterials (Dabrunz et al. 2011; Karimi et al. 2018), and 2) instead of fluorescent tubes, UV fluorescent tubes (Magic Sun 23/160 R 160 W; UVA output 44 W, UVB output 1.1%, measured with an RM12 radiometer; Dr. Göbel UV-Electronic) were used as a light source, applying an 8:16-h light:dark rhythm.

As test medium, the vitamin- and selenium-enriched culture medium without seaweed extract was used (see section *Test organism*). For each acute toxicity test, one replicate consisted of 5 juvenile *Daphnia* (age <24 h), exposed to the respective pesticide concentration, test series, and UVA radiation (=treatment), and each treatment was replicated 4 times. Each day daphnids were visually checked for their immobility (i.e., after 24, 48, 72, and 96 h of exposure). Immobility data were used to calculate the pesticides' 96-h median effect concentration (EC50) values for the respective exposure scenarios.

We chose seaweed extract as the NOM representative, given its recommendation in standard test guidelines as an additive for long-term culturing of *D. magna* and chronic *Daphnia* experiments (Organisation for Economic Co-operation and Development 2008). Prior to application, an seaweed extract subsample (8 mg TOC/L, diluted in 50 mL test medium,

TABLE 3: Applied exposure scenarios for the acute toxicity bioassays (see *Bioassay setup*)^a

Test series	UVA level	UV radiation ^b (W UVA/m ²)	nTiO ₂ (µg/L)	NOM (mg TOC/L)
PEST	UVA-I	0	0	0
	UVA-II	0.4–0.6	0	0
	UVA-III	1–1.4	0	0
	UVA-IV	2.2–2.6	0	0
PEST + nTiO ₂	UVA-I	0	50	0
	UVA-II	0.4–0.6	50	0
	UVA-III	1–1.4	50	0
	UVA-IV	2.2–2.6	50	0
PEST + NOM	UVA-I	0	0	4
	UVA-II	0.4–0.6	0	4
	UVA-III	1–1.4	0	4
	UVA-IV	2.2–2.6	0	4
PEST + nTiO ₂ + NOM	UVA-I	0	50	4
	UVA-II	0.4–0.6	50	4
	UVA-III	1–1.4	50	4
	UVA-IV	2.2–2.6	50	4

^aEach scenario was applied to each of the 6 pesticides.

^bBefore the start of the experiments, UVA radiation was measured at the water surface of the test vessels, which were randomly placed in the areas that were in the UV range listed (see *Bioassay setup*).

NOM = natural organic matter; nTiO₂ = nano-sized titanium dioxide; PEST = pesticide.

pesticide- and nTiO₂-free) was analyzed as part of an earlier study at DOC-LABOR (Karlsruhe, Germany), providing a more detailed characterization (contains data per Seitz et al. 2016; Supplemental Data, Table S1).

Chemical analysis

We were aiming to unveil the influence of nTiO₂, UVA radiation, and NOM on the degradation and therefore possible alteration of acute pesticide toxicity over the course of the experiments. Therefore, water samples were taken at the highest applied pesticide concentration for each exposure scenario right after the pesticide application (0 h), as well as after the termination of the experiments (96 h). Samples (10 mL) were stored in glass vials (20 mL) at –20 °C until realizing analysis via ultra-high-performance liquid chromatography (Thermo Fischer Scientific). Prior to the measurements, samples were centrifuged to exclude any undissolved particles. By doing so, also pesticides that might have been adsorbed onto the dispersed ENM were separated from the dissolved fraction. The concentrations were determined using an external standard calibration applying matrix-aligned standards. Samples of parathion and permethrin experiments could not be confirmed analytically. Therefore, interpretation and discussion of the observed effects for these 2 pesticides are based on nominal data and existing literature.

Data analysis

After 96 h of exposure, immobility data of each of the treatment combinations were used to calculate EC50 values (Supplemental Data, Table S2), which is the concentration of the respective pesticide, that caused immobility in 50% of the test organisms. This was done by fitting adequate dose-response models (Ritz and Streibig 2005). The most

appropriate model was selected based on Akaike's information criterion and visual judgement (Supplemental Data, Figure S2 and Table S2). Statistical significance between EC50 values among the different exposure scenarios was tested by applying Bonferroni-adjusted confidence interval testing (Wheeler et al. 2006). The 96-h EC50s referred to in the following sections are based on nominal applied concentrations, if not explicitly stated otherwise. Interpretation of these EC50s is based on changes in the toxicity of the applied pesticide, implying the degradation of the respective parent compound and formation of potential by-products. In addition, 96-h EC50s based on measured concentrations were calculated and are available in the Supplemental Data (Table S2 and Figure S3).

RESULTS

Azoxystrobin

In the absence of NOM and nTiO₂ (PEST), increasing UVA radiation did not have a significant impact on azoxystrobin toxicity, with 96-h EC50 values ranging between 180 and 240 µg/L (UVA-I and UVA-III, respectively; Figure 1). There was also no meaningful photo-induced degradation of azoxystrobin over 96 h (Table 4), except for UVA-IV (~20% relative to 0 h). In PEST + nTiO₂, a UVA radiation ≥UVA-III caused an up to 1.6-fold decrease in azoxystrobin toxicity. This is in accordance with the measured azoxystrobin concentrations, showing an approximately 15% reduction at UVA-IV after 96 h compared to UVA-I (Table 4). At low UVA radiation, PEST + NOM revealed generally an up to 2-fold reduced azoxystrobin toxicity relative to the other test series (Figure 1). However, PEST + NOM caused a significantly (up to ~1.4-fold) enhanced toxicity starting with the UVA-III treatment (UVA-III, 210 µg/L, and UVA-IV, 205 µg/L), relative to the absence of UV (290 µg/L; Figure 1). This contradicts the measured azoxystrobin concentrations showing an approximately 25% higher degradation relative to

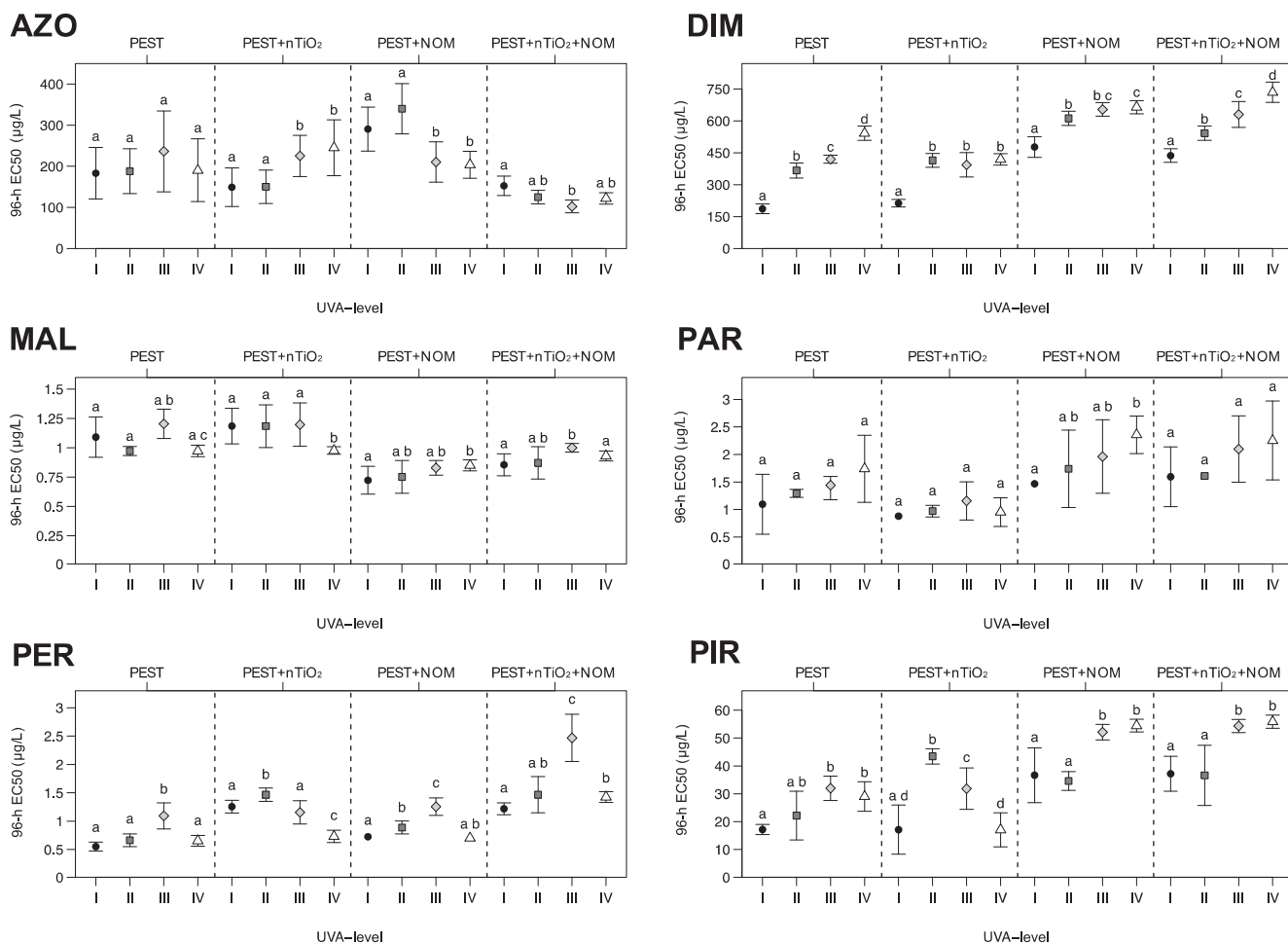


FIGURE 1: Median effect concentrations at 96 h ($\pm 95\%$ confidence interval) of *Daphnia magna* for the 6 pesticides azoxystrobin, dimethoate, malathion, parathion, permethrin, and pirimicarb based on nominal concentrations, under varying levels of UVA radiation (I = 0.00; II = 0.40–0.60; III = 1.00–1.40; and IV = 2.20–2.60 W UVA/m²) and test series (PEST, PEST + nTiO₂, PEST + NOM, and PEST + nTiO₂ + NOM; Table 3). For more information on the applied pesticides and concentrations, see Table 1. Different letters denote statistically significant differences between individual UVA levels but within one test series. AZO = azoxystrobin; DIM = dimethoate; EC50 = median effect concentration; MAL = malathion; NOM = natural organic matter; nTiO₂ = nano-sized titanium dioxide; PAR = parathion; PER = permethrin; PEST = pesticide; PIR = pirimicarb.

UV-I (Table 4). When combining PEST + nTiO₂ + NOM, increasing UVA radiation led to the highest observed azoxystrobin toxicity among the 4 test series. At UVA-III and UVA-IV, the 96-h EC50 values were significantly reduced by 1.25- and 1.5-fold (UVA-III, 100 µg/L, and UVA-IV, 120 µg/L, respectively) relative to UVA-I (150 µg/L; Figure 1) and despite an approximately 25% azoxystrobin degradation after 96 h.

Dimethoate

The absence of NOM and nTiO₂ (PEST) revealed a continuous decrease of dimethoate toxicity with increasing UVA radiation, with the 96-h EC50 value increasing up to 3-fold from approximately 185 to 540 µg/L (Figure 1). In the presence of nTiO₂, the toxicity of dimethoate decreased approximately 2-fold by increasing UVA radiation from UVA-I to UVA-II (96-h EC50, ~210 and 415 µg/L, respectively; Figure 1) but reached a plateau and did not further decrease at higher UVA levels. Similarly, PEST + NOM showed generally lower dimethoate

toxicity (factor of ~1.7 relative to PEST + nTiO₂), leading to 96-h EC50s of up to 660 µg/L (Figure 1). Also, in the PEST + nTiO₂ + NOM test series, toxicity was reduced with increasing UVA (Figure 1). The lowest dimethoate degradation was observed in test series PEST with a maximum of approximately 10%, despite the up to 3-fold observed toxicity reduction (0 vs 96 h at UVA-IV). For PEST + nTiO₂, PEST + NOM, and PEST + nTiO₂ + NOM, the concentration of dimethoate was reduced by up to 30% (Table 4).

Malathion

Increasing UVA radiation alone did not change malathion 96-h EC50 values meaningfully; they fluctuated by a factor of 1.2 (Figure 1). The test series PEST + nTiO₂ influenced malathion toxicity to a similar extent (1.2-fold), but this impact was statistically significant at the highest UVA level (Figure 1). In the presence of NOM, malathion toxicity was enhanced compared to PEST and PEST + nTiO₂ with increasing 96-h EC50 at higher

TABLE 4: Measured concentrations of azoxystrobin, dimethoate, malathion, and pirimicarb in test series 1–4 at varying UVA radiation levels (I–IV), approximately 10 min (0 h) after pesticide application to the respective test medium and exposure scenario, as well as after the termination of the experiments (96 h)^a

Test series	UVA	Time (h)	AZO (µg/L)	△ (%)	DIM (µg/L)	△ (%)	MAL (µg/L)	△ (%)	PIR (µg/L)	△ (%)
PEST	—	0	541	—	2900	—	6.3	—	69.6	—
	I	96	590	9	2862	–1	2.0	–68	80.7	16
	II	96	593	10	2633	–9	2.7	–58	67.6	–3
	III	96	545	1	2688	–7	2.1	–66	30.0	–57
	IV	96	435	–20	2532	–13	2.0	–68	14.6	–79
PEST + nTiO ₂	—	0	542	—	2856	—	2.6	—	64.7	—
	I	96	527	–3	2827	–1	1.3	–48	91.9	42
	II	96	642	18	2804	–2	2.2	–14	7.0	–89
	III	96	630	16	2946	3	1.1	–58	<LOQ	NA
	IV	96	459	–15	1983	–31	0.9	–65	<LOQ	NA
PEST + NOM	—	0	515	—	2989	—	4.4	—	35.6	—
	I	96	477	–7	2798	–6	3.2	–29	43.0	21
	II	96	601	17	2887	–3	3.1	–29	22.7	–36
	III	96	607	18	2652	–11	2.9	–35	17.5	–51
	IV	96	378	–27	2150	–28	3.2	–29	9.2	–74
PEST + nTiO ₂ + NOM	—	0	507	—	2981	—	2.9	—	37.0	—
	I	96	555	9	2837	–5	2.1	–30	38.8	5
	II	96	609	20	2841	–5	2.0	–31	29.4	–20
	III	96	460	–9	2700	–9	2.2	–25	13.8	–63
	IV	96	377	–26	2028	–32	0.9	–71	4.4	–88

^aThe parathion and permethrin samples could not be analyzed and are therefore not listed. △ illustrates the relative degradation as a percentage after 96 h, referring to the 0-h concentrations of the respective test series, whereas negative values indicate pesticide degradation. Please note that increased levels of AZO and pirimicarb after 96 h relative to 0 h are likely driven by evaporation of the test medium, consequently leading to a concentration of the pesticide in the remaining medium.

AZO = azoxystrobin; DIM = dimethoate; LOQ = limit of quantification; MAL = malathion; NA = not assessable; NOM = natural organic matter; nTiO₂ = nano-sized titanium dioxide; PEST = pesticide; PIR = pirimicarb.

UVA radiation, which was partly significant (Figure 1). Similarly, PEST + nTiO₂ + NOM revealed a tendency toward reduced malathion toxicity relative to PEST + NOM (up to ~1.2-fold; Figure 1). The malathion concentration decreased over the study duration, a pattern enhanced by increasing UVA radiation, with the lowest decrease in the presence of nTiO₂ alone (30%) and the highest in the other test series (70%).

Parathion

Increasing UVA radiation alone induced a non-significant trend of reduced parathion toxicity by up to 70% (Figure 1). Compared to the PEST only treatment, parathion toxicity was generally higher in the presence of nTiO₂ by a factor between 1.2- and 1.8-fold (comparing the respective UVA levels of both test series). Nonetheless, in PEST + nTiO₂ the 96-h EC50 increased from approximately 0.85 µg/L at UVA-I to approximately 1.15 µg/L at UVA-III, followed by a decrease to 0.95 µg/L at UVA-IV (Figure 1). Even if not statistically significant, the presence of NOM in both PEST + NOM and PEST + nTiO₂ + NOM favored the lowest observed parathion toxicity, further decreasing with enhancing UVA radiation (Figure 1).

Permethrin

In the absence of nTiO₂ or NOM, UVA levels led to a significant decrease of permethrin toxicity by a factor of 2 at UVA-III, followed by a recurring decrease at UVA-IV to nearly the same level as observed at UVA-I (Figure 1). A similar pattern

was observed in the presence of nTiO₂ (PEST + nTiO₂; Figure 1). The addition of NOM (PEST + NOM) promoted the mitigation of permethrin toxicity at UVA-I and UVA-II by a factor of approximately 1.3, relative to the absence of NOM. Compared to PEST + nTiO₂, however, the 96-h EC50s of PEST + NOM at UVA-I and UVA-II were approximately 1.7-fold lower, a pattern which was not confirmed for UVA-III and UVA-IV (Figure 1). Combining PEST + nTiO₂ + NOM induced a 2.2-fold reduced permethrin toxicity relative to PEST.

Pirimicarb

With increased UVA radiation but in the absence of nTiO₂ and NOM (PEST), pirimicarb toxicity decreased by up to approximately 1.9-fold, which was partly significant (Figure 1). In the presence of nTiO₂, pirimicarb toxicity was decreased at lower UVA radiation, whereas this impact vanished at the highest UVA radiation tested (Figure 1). The presence of NOM irrespective of the nTiO₂ presence and UVA radiation revealed the highest reduction in pirimicarb toxicity. These patterns in toxicity were confirmed by chemical analysis, with decreasing pirimicarb concentrations at increasing UVA radiation. This decrease was up to 90% (UVA-IV; Table 4).

DISCUSSION

Influence of UVA illumination (PEST)

In the present study, UVA illumination of the pesticides resulted in 2 effect patterns: 1) decreasing pesticide toxicity with

increasing UVA illumination, and 2) constant pesticide toxicity independent of the applied UVA radiation.

Decreasing pesticide toxicity with increasing UVA illumination was hypothesized for substances with high photolytic potential as represented by a low p-DT50, a pattern which was observed for dimethoate, parathion, and pirimicarb. In principle, the reduction of dimethoate and pirimicarb toxicity was confirmed by chemical analysis; dimethoate and pirimicarb concentrations were substantially reduced by up to approximately 15 and 80%, respectively (Table 4). These observations are in line with earlier studies with dimethoate (Evgenidou et al. 2006) and pirimicarb (e.g., Schwack and Kopf 1993; Romero et al. 1994; Pirisi et al. 1996; Seitz et al. 2012), highlighting a more efficient photodegradation for pirimicarb. Moreover, Zoh et al. (2006) highlighted an 80% reduction in parathion under natural solar radiation (average intensity 6.4–19 W/m²) within 150 min, confirming its photolytic properties (see also Table 1). Hence, the reduction in parathion toxicity reported in the present study is likely driven by its photolysis, though it is less efficient relative to pirimicarb and dimethoate. Still, we were not able to confirm this assumption by chemical analyses of the parathion samples.

Consistent pesticide toxicity regardless of the applied UVA radiation was observed for azoxystrobin, malathion, and permethrin, suggesting no detoxification. The degradation of azoxystrobin was up to 20% with increasing UVA illumination (Table 4). Indeed, the UV-visible absorption spectrum of azoxystrobin slightly overlaps with the solar light spectrum, suggesting that UV-induced photodegradation could occur under natural conditions (Boudina et al. 2007). In contrast to azoxystrobin, malathion was even in darkness (UVA-I) degraded by up to approximately 70% (Table 4), suggesting hydrolysis as a dominating detoxification pathway with little additional impact through photolysis (Table 1). For permethrin we would have assumed a fast degradation in the presence of UVA followed by significant detoxification, given the low p-DT50 of 1 d. The mostly steady 96-h EC50 with increasing UV radiation could be driven by “knock down” through fast interference with sodium channels, leading to rapid paralysis and finally resulting in death, a mode of action typical for pyrethroids such as permethrin (US Environmental Protection Agency 2006; Ensley 2007). Consequently, the responses of the test organisms to permethrin exposure may have occurred faster than any potential degradation.

Influence of UVA illumination + nTiO₂ (PEST + nTiO₂)

Combining UVA radiation with nTiO₂ resulted in 3 patterns: 1) enhanced pesticide degradation compared to nTiO₂ absence, along with toxicity reduction; 2) low UVA radiation induced a reduction, whereas high UVA radiation enhanced toxicity; and 3) steady 96-h EC50s despite increasing UVA radiation, whereas the toxicity was generally higher compared to nTiO₂ absence (PEST).

In the present study, more efficient pesticide degradation in the presence versus absence of nTiO₂ was observed for

dimethoate (PEST 13% vs PEST + nTiO₂ 31%; UVA-IV) and pirimicarb (PEST 79% vs PEST + nTiO₂ < limit of quantification [LOQ]; UVA-IV), being partly accompanied by additional detoxification. An amplified degradation is known to be triggered by solar illumination of a co-occurring photocatalyst like nTiO₂, inducing various redox reactions (Konstantinou and Albanis 2003). This results in the formation of ROS (Turchi and Ollis 1989; Low et al. 1991; Pelizzetti and Minero 1999), finally leading to mineralization and detoxification of organic compounds such as pesticides (Hoffmann et al. 1995; Robert and Malato 2002).

Solar illumination of a co-occurring photocatalyst has been documented as efficient treatment technology for organic micropollutants in general and for pesticides, including azoxystrobin, dimethoate, and pirimicarb, in particular. However, those studies mainly focused on environmentally irrelevant concentrations of photocatalysts (milligrams to grams per liter range) and UV radiation that may be considered rather high (up to 30 W/m²; see Malato et al. 2001; Kim et al. 2006; Chen et al. 2007; Navarro et al. 2009). Our observations are largely in line with those studies and furthermore demonstrate that photocatalytic degradation and detoxification of pesticides take place even under conditions very close to concentrations considered field-relevant (i.e., 50 µg nTiO₂/L; Figure 1). Moreover, the lower p-DT50 seemed to promote the degradation efficiency of pirimicarb (0.5–6 d; up to <LOQ), relative to dimethoate (175 d; up to 30%).

On the downside, the presence of nTiO₂ at higher UVA radiation also resulted in increased toxicity in *D. magna* as demonstrated for malathion, permethrin, and pirimicarb (Figure 1) despite elevated pesticide degradation (measured for malathion and pirimicarb samples; Table 4). Pesticides malathion, permethrin, and pirimicarb act as acetylcholinesterase inhibitors, which is known to be a fast-acting mode of action (Cambon et al. 1979; Xuereb et al. 2009). This, in combination with the highest applied UVA radiation along with the presence of nTiO₂, might have facilitated the pesticide degradation but potentially resulted in synergistic stress (through ROS), causing increased toxicity while outweighing degradation-triggered detoxification. In support of this assumption, Johnson et al. (2015) observed sublethal toxicity of nTiO₂ when illuminated with UVA radiation in the eastern oyster (*Crassostrea virginica*) at a concentration as low as 50 µg/L (sensu Amiano et al. 2012).

The 96-h EC50s of dimethoate that indicate higher toxicity at test series PEST + nTiO₂ than at test series PEST despite more efficient degradation (Table 4) could, in addition, be induced by the formation of metabolites that are more toxic than the parent substance (Evgenidou et al. 2006; Farner Budarz et al. 2017). It was shown that during photocatalytic degradation with nTiO₂, dimethoate is degraded into 9 by-products (Evgenidou et al. 2006), whereas the major by-product, ome-thoate (Van Scoy et al. 2016), is 90-fold more toxic than the mother compound (Pesticide Properties Database; Lewis et al. 2016). Likewise, the photocatalysis (UV = 5.8 W/m²; TiO₂ = 120 mg/L) of malathion sharply increases its toxicity toward *Vibrio fischeri*, whereas no increase in toxicity was

observed when treating malathion with UV alone (Li et al. 2019). Hence, also for malathion, a formation of toxic by-products at the highest applied UVA radiation seems likely.

With a medium p-DT50 of 30 d, parathion might have been subjected to photolytic degradation in the presence of UVA, which was shown to be significantly amplified in the presence of the photocatalyst nTiO₂ (Evgenidou et al. 2007). However, photocatalytic transformation of parathion can lead to the formation of paraoxon (Evgenidou et al. 2007). Paraoxon's acute toxicity toward *D. magna* is approximately 10 times higher relative to the parent compound (Guilhermino et al. 1996), being the potential trigger for the increased parathion toxicity in test series PEST + nTiO₂ compared to test series PEST. The latter, however, was not analytically confirmed. Furthermore, adsorption of the pesticide onto nTiO₂ (which was not quantified during the present study), followed by ingestion of the ENM might have favored pesticide accumulation in the digestive system of *D. magna*, potentially leading to an enhanced toxicity. Accumulation of ENMs in *Daphnia* was recently demonstrated by Mao et al. (2016). Similarly, pesticide adsorption onto ENMs was assessed in a study by Momic et al. (2016) describing the adsorption of an organophosphate on gold nanospheres and nanorods. Still, we believe that substantial adsorption would require a relatively high surface area during the interaction time. At the applied concentrations of nTiO₂ in the low micrograms per liter range, we do not expect substantial pesticide adsorption onto nTiO₂ particles. This assumption, however, was not evaluated as part of the pesticide measurements conducted for the present study but is supported by recent work with metal ions (R. Roy et al., unpublished manuscript, University of Koblenz-Landau, Landau, Germany).

In essence, we demonstrated a distinctive impact of field-relevant UVA radiation (up to 2.6 W UVA/m²) on nTiO₂-induced toxicity applied at very low, and thus field-relevant, concentrations. Effects induced by UVA and nTiO₂ were observed at radiation intensities and concentrations 2.5- to 300-fold and 4- to 2000-fold, respectively, lower than applied in existing studies (e.g., Romero et al. 1994; Zoh et al. 2006; Evgenidou et al. 2007; Seitz et al. 2012). Our observations seem to be triggered by a combination of nTiO₂ exerting direct negative effects on aquatic biota (i.e., formation of ROS [Amiano et al. 2012]) and an alteration of the toxic potential of co-occurring pesticides. The latter might either be reduced toxicity as a consequence of elevated photolytic degradation or increased toxicity induced by the formation of toxic by-products. Furthermore, this impact seems partly explained by the pesticides' physicochemical properties (i.e., p- and h-DT50).

Influence of UVA illumination in the presence of NOM (PEST + nTiO₂ + NOM)

The application of NOM resulted in 2 contrasting patterns: 1) reduced pesticide toxicity in the presence of NOM, not accompanied by an enhanced pesticide degradation, and 2) NOM-induced inhibition in pesticide degradation, increasing

pesticide toxicity on a relative scale. This is not in line with our expectations because we hypothesized that NOM would amplify the degradation and therefore detoxification of pesticides. Furthermore, there was no clear observable relationship between K_{OC} and degradation efficiency or detoxification. More precisely, higher adsorption tendencies toward NOM, triggered by comparably high K_{OC}s did not reveal a specific impact on the pesticides' degradation or toxicity (Table 4; Supplemental Data, Table S2).

The generally detoxifying effect of NOM was observed for dimethoate, parathion, and pirimicarb (relative to PEST, and PEST + nTiO₂; Figure 1), which could not be linked to a higher pesticide degradation for dimethoate and pirimicarb (Table 4). The lower pesticide toxicity seems, hence, driven by the potential of NOM to serve as an energy source with a positive effect on the fitness of *D. magna* because NOM increases the life span and offspring along with a higher tolerance toward other stressors (Bouchnak and Steinberg 2010; Bergman Filho et al. 2011). In addition to an increased fitness and stress tolerance of *D. magna*, NOM could directly interact with the pesticide by adsorption, reducing the dissolved pesticide concentration and consequently bioavailability (Yang et al. 2006). Moreover, NOM is prone to transformations induced by light (Sulzberger and Durisch-Kaiser 2009) potentially triggered by photoreactive intermediates originating from illuminated ENMs such as nTiO₂ (Aiken et al. 2011). This will most likely have an influence on nTiO₂-mediated photocatalytic reactions (i.e., the formation of ROS [Ma et al. 2012; Kim et al. 2013]), and consequently the detoxification of micropollutants (Bundschuh 2011), demonstrated by the degradation efficiency and resulting detoxification of dimethoate being most effective in the presence of nTiO₂ and NOM.

In contrast, absorption of UVA radiation by NOM could lead to a UVA-attenuating shading effect (Albrektienė et al. 2012), decreasing the photolysis/photocatalysis potential of certain pesticides indirectly (Garbin et al. 2007). The apparently increased toxicity of malathion in the presence of NOM may, thus, be based on a shading-triggered decreased UVA availability for photolysis, consequently leading to the reduced potential for pesticide degradation or the formation of less toxic metabolites. This is a mechanism that has also been suggested for the biocide fipronil (Bejarano et al. 2005). While acting as a light-absorbing entity, NOM is also suggested to induce the formation of reactive intermediates (e.g., ROS [Garbin et al. 2007; Aiken et al. 2011]) that are known to be toxic for aquatic life (Cabiscol et al. 2000; Buonocore et al. 2010).

CONCLUSION

The present study shows that exposing pesticides to degradation-promoting factors like UV radiation, nTiO₂, and NOM at field-relevant conditions does not necessarily lead to their detoxification. Whereas existing studies are mainly focusing on detoxifying pretreatments of contaminated waters (e.g., Zoh et al. 2006; Seitz et al. 2012), the present study is

among the first to address the direct impact of a more complex field-relevant setup on the inherent toxicity of pesticides (cf. Farner Budarz 2017). We conclude that the impact on the resulting ecotoxicological potential of the pesticide seems mainly driven by the specific treatment process, that is, photolysis versus photocatalysis (Li et al. 2019), rather than by physicochemical properties, such as photo- and hydrolytic stability. In nature, the detoxification of those micropollutants seems strongly affected by the presence of NOM (Garbin et al. 2007; Aiken et al. 2011). More specifically, the presence of NOM potentially amplifies the detoxification of pesticides, on the one hand, by facilitating photocatalytic degradation. On the other hand, photocatalytic degradation might also enhance the ecotoxicological potential, possibly because of the formation of degradation compounds that are more toxic than the parent compound. The combined impacts of UVA, photoactive ENMs, and NOM on pesticide toxicity seem therefore not easily predictable.

Supplemental Data—The Supplemental Data are available on the Wiley Online Library at <https://doi.org/10.1002/etc.4851>.

Acknowledgment—We express our sincere gratitude to T. Bürgi, F. Seitz, R. Rosenfeldt, R. Roy, and T. Schmitt for support in the laboratory during the course of the present study. The present study is part of the research group INTERNANO, supported by the German Research Foundation (SCHU2271/5-2) and by funding from the Ministry of Science Rhineland-Palatinate. We thank the European Fund for regional development for the financial support of the PHOTOPUR project, which is performed within the framework of Interreg V and the Science Offensive. Open access funding enabled and organized by Projekt DEAL.

Disclaimer—The authors declare no conflict of interest.

Data Availability Statement—Data, associated metadata, and calculation tools are available from the corresponding author (bunds Schuh@uni-landau.de).

REFERENCES

- Aiken GR, Hsu-Kim H, Ryan JN. 2011. Influence of dissolved organic matter on the environmental fate of metals, nanoparticles, and colloids. *Environ Sci Technol* 45:3196–3201.
- Albrektienė R, Rimeika M, Zalieckienė E, Šaulys V, Zagorskis A. 2012. Determination of organic matter by UV absorption in the ground water. *J Environ Eng Landsc Manag* 20:163–167.
- Amiano I, Olabarrieta J, Vitorica J, Zorita S. 2012. Acute toxicity of nano-sized TiO₂ to *Daphnia magna* under UVA irradiation. *Environ Toxicol Chem* 31:2564–2566.
- ASTM International. 2007. Standard guide for conducting acute toxicity tests on test materials with fishes, macroinvertebrates, and amphibians. E729-96. In *Annual Book of ASTM Standards*, Vol. 11.06. Philadelphia, PA, USA, pp 1–22.
- Bar-Ilan O, Chuang CC, Schwahn DJ, Yang S, Joshi S, Pedersen JA, Hamers RJ, Peterson RE, Heideman W. 2013. TiO₂ nanoparticle exposure and illumination during zebrafish development: Mortality at parts per billion concentrations. *Environ Sci Technol* 47:4726–4733.
- Bejarano AC, Chandler GT, Decho AW. 2005. Influence of natural dissolved organic matter (DOM) on acute and chronic toxicity of the pesticides chlorothalonil, chlorpyrifos and fipronil on the meiobenthic estuarine copepod *Amphiascus tenuiremis*. *J Exp Mar Biol Ecol* 321:43–57.
- Bergman Filho T, Soares A, Loureiro S. 2011. Energy budget in *Daphnia magna* exposed to natural stressors. *Environ Sci Pollut Res* 18:655–662.
- Bouchnak R, Steinberg CEW. 2010. Modulation of longevity in *Daphnia magna* by food quality and simultaneous exposure to dissolved humic substances. *Limnologica* 40:86–91.
- Boudina A, Emmelin C, Baaliouamer A, Paissé O, Chovelon JM. 2007. Photochemical transformation of azoxystrobin in aqueous solutions. *Chemosphere* 68:1280–1288.
- Bunds Schuh M, Zubrod JP, Seitz F, Stang C, Schulz R. 2011. Ecotoxicological evaluation of three tertiary wastewater treatment techniques via meta-analysis and feeding bioassays using *Gammarus fossarum*. *J Hazard Mater* 192:772–778.
- Buonocore G, Perrone S, Tataranno ML. 2010. Oxygen toxicity: Chemistry and biology of reactive oxygen species. *Semin Fetal Neonatal Med* 15:186–190.
- Cabiscol E, Tamarit J, Ros J. 2000. Oxidative stress in bacteria and protein damage by reactive oxygen species. *Int Microbiol* 3:3–8.
- Cambon C, Declume C, Derache R. 1979. Effect of the insecticidal carbamate derivatives (carbofuran, pirimicarb, aldicarb) on the activity of acetylcholinesterase in tissues from pregnant rats and fetuses. *Toxicol Appl Pharmacol* 49:203–208.
- Chen JQ, Wang D, Zhu MX, Gao CJ. 2007. Photocatalytic degradation of dimethoate using nanosized TiO₂ powder. *Desalination* 207:87–94.
- Dabrunz A, Duester L, Prasse C, Seitz F, Rosenfeldt R, Schilde C, Schaumann GE, Schulz R. 2011. Biological surface coating and molting inhibition as mechanisms of TiO₂ nanoparticle toxicity in *Daphnia magna*. *PLoS One* 6:e20112.
- Ensley S. 2007. Pyrethrins and pyrethroids. In Gupta RC, ed, *Veterinary Toxicology: Basic and Clinical Principles*. Academic, New York, NY, USA, pp 494–498.
- Evgenidou E, Konstantinou I, Fytianos K, Albanis T. 2006. Study of the removal of dichlorvos and dimethoate in a titanium dioxide mediated photocatalytic process through the examination of intermediates and the reaction mechanism. *J Hazard Mater* 137:1056–1064.
- Evgenidou E, Konstantinou I, Fytianos K, Poulous I, Albanis T. 2007. Photocatalytic oxidation of methyl parathion over TiO₂ and ZnO suspensions. *Catal Today* 124:156–162.
- Farner Budarz J, Cooper EM, Gardner C, Hodzic E, Ferguson PL, Gunsch CK, Wiesner MR. 2017. Chlorpyrifos degradation via photoreactive TiO₂ nanoparticles: Assessing the impact of a multi-component degradation scenario. *J Hazard Mater* 372:61–68.
- Garbin JR, Milori DMBP, Simões ML, da Silva WTL, Neto LM. 2007. Influence of humic substances on the photolysis of aqueous pesticide residues. *Chemosphere* 66:1692–1698.
- Garg S, Rose AL, Waite TD. 2011. Photochemical production of superoxide and hydrogen peroxide from natural organic matter. *Geochim Cosmochim Acta* 75:4310–4320.
- Gondikas AP, von der Kammer F, Reed RB, Wagner S, Ranville JF, Hofmann T. 2014. Release of TiO₂ nanoparticles from sunscreens into surface waters: A one-year survey at the old Danube recreational lake. *Environ Sci Technol* 48:5415–5422.
- Gottschalk F, Nowack B. 2011. The release of engineered nanomaterials to the environment. *J Environ Monit* 13:1145–1155.
- Gottschalk F, Sun T, Nowack B. 2013. Environmental concentrations of engineered nanomaterials: Review of modeling and analytical studies. *Environ Pollut* 181:287–300.
- Guilhermino L, Lopes MC, Carvalho AP, Soared AMVM. 1996. Inhibition of acetylcholinesterase activity as effect criterion in acute tests with juvenile *Daphnia magna*. *Chemosphere* 32:727–738.
- Häder DP, Lebert M, Schuster M, del Campo L, Helbling EW, McKenzie R. 2007. ELDONET—A decade of monitoring solar radiation on five continents. *Photochem Photobiol* 83:1348–1357.
- Hariharan C. 2006. Photocatalytic degradation of organic contaminants in water by ZnO nanoparticles: Revisited. *Appl Catal A Gen* 304:55–61.
- Hoffmann MR, Martin ST, Choi W, Bahnemann DW. 1995. Environmental applications of semiconductor photocatalysis. *Chem Rev* 95:69–96.
- Johnson BD, Gilbert SL, Khan B, Carroll DL, Ringwood AH. 2015. Cellular responses of eastern oysters, *Crassostrea virginica*, to titanium dioxide nanoparticles. *Mar Environ Res* 111:135–143.

- Karimi S, Troeung M, Wang R, Draper R, Pantano P. 2018. Acute and chronic toxicity of metal oxide nanoparticles in chemical mechanical planarization slurries with *Daphnia magna*. *Environ Sci Nano* 5: 1670–1684.
- Keller AA, Lazareva A. 2014. Predicted releases of engineered nanomaterials: From global to regional to local. *Environ Sci Technol Lett* 1:65–70.
- Kim C, Park H-j, Cha S, Yoon J. 2013. Facile detection of photogenerated reactive oxygen species in TiO₂ nanoparticles suspension using colorimetric probe-assisted spectrometric method. *Chemosphere* 93:2011–2015.
- Kim TS, Kim JK, Choi K, Stenstrom MK, Zoh KD. 2006. Degradation mechanism and the toxicity assessment in TiO₂ photocatalysis and photolysis of parathion. *Chemosphere* 62:926–933.
- Konstantinou IK, Albanis TA. 2003. Photocatalytic transformation of pesticides in aqueous titanium dioxide suspensions using artificial and solar light: Intermediates and degradation pathways. *Appl Catal B* 42: 319–335.
- Lewis KA, Tzilivakis J, Warner DJ, Green A. 2016. An international database for pesticide risk assessments and management. *Hum Ecol Risk Assess* 22:1050–1064.
- Li W, Zhao Y, Yan X, Duan J, Saint CP, Beecham S. 2019. Transformation pathway and toxicity assessment of malathion in aqueous solution during UV photolysis and photocatalysis. *Chemosphere* 234:204–214.
- Low GKC, McEvoy SR, Matthews RW. 1991. Formation of nitrate and ammonium ions in titanium dioxide mediated photocatalytic degradation of organic compounds containing nitrogen atoms. *Environ Sci Technol* 25:460–467.
- Lüderwald S, Dackermann V, Seitz F, Adams E, Feckler A, Schilde C, Schulz R, Bundschuh M. 2019. A blessing in disguise? Natural organic matter reduces the UV light-induced toxicity of nanoparticulate titanium dioxide. *Sci Total Environ* 663:518–526.
- Ma H, Brennan A, Diamond SA. 2012. Photocatalytic reactive oxygen species production and phototoxicity of titanium dioxide nanoparticles are dependent on the solar ultraviolet radiation spectrum. *Environ Toxicol Chem* 31:2099–2107.
- Malato S, Caceres J, Aguera A, Mezcuca M, Hernando D, Vial J, Fernandez-Alba AR. 2001. Degradation of imidacloprid in water by photo-fenton and TiO₂ photocatalysis at a solar pilot plant: A comparative study. *Environ Sci Technol* 35:4359–4366.
- Mao L, Liu C, Lu K, Su Y, Gu C, Huang Q, Petersen EJ. 2016. Exposure of few layer graphene to *Limnodrilus hoffmeisteri* modifies the graphene and changes its bioaccumulation by other organisms. *Carbon* 109:566–574.
- Momic T, Pasti TL, Bogdanovic U, Vodnik V, Mrakovic A, Rakocevic Z, Vasic V, Pavlovic VB. 2016. Adsorption of organophosphate pesticide dimethoate on gold nanospheres and nano rods. *J Nanomater* 2016: 8910271.
- National Center for Biotechnology Information. 2019a. PubChem compound summary for CID 3082, Dimethoate. [cited 2019 June 9]. Available from: <https://pubchem.ncbi.nlm.nih.gov/compound/Dimethoate>
- National Center for Biotechnology Information. 2019b. PubChem compound summary for CID 31645, Pirimicarb. [cited 2019 June 9]. Available from: <https://pubchem.ncbi.nlm.nih.gov/compound/Pirimicarb>
- Navarro S, Fenoll J, Vela N, Ruiz E, Navarro G. 2009. Photocatalytic degradation of eight pesticides in leaching water by use of ZnO under natural sunlight. *J Hazard Mater* 172:1303–1310.
- Organisation for Economic Co-operation and Development. 2004. Test No. 202: *Daphnia* sp. acute immobilisation test. *OECD Guidelines for Testing of Chemicals*. Paris, France.
- Organisation for Economic Co-operation and Development. 2008. Test No. 211: *Daphnia magna* reproduction test. *OECD Guidelines for Testing of Chemicals*. Paris, France.
- Ouyang W, Santiago ARP, Cerdán-Gómez K, Luque R. 2019. Nanoparticles within functional frameworks and their applications in photo(electro) catalysis. In Prieto JP, Béjar MG, eds, *Photoactive Inorganic Nanoparticles: Surface Composition and Nanosystem Functionality*. Elsevier, Amsterdam, The Netherlands, pp 109–138.
- Pelizzetti E, Minero C. 1999. Role of oxidative and reductive pathways in the photocatalytic degradation of organic compounds. *Colloids Surf A Physicochem Eng Asp* 151:321–327.
- Peters RJB, van Bommel G, Milani NBL, den Hertog GCT, Undas AK, van der Lee M, Bouwmeester H. 2018. Detection of nanoparticles in Dutch surface waters. *Sci Total Environ* 621:210–218.
- Piccinno F, Gottschalk F, Seeger S, Nowack B. 2012. Industrial production quantities and uses of ten engineered nanomaterials in Europe and the world. *J Nanopart Res* 14:1109.
- Pirisi FM, Cabras P, Garau VL, Melis M, Secchi E. 1996. Photodegradation of pesticides. Photolysis rates and half-life of pirimicarb and its metabolites in reactions in water and in solid phase. *J Agric Food Chem* 44:2417–2422.
- Ritz C, Streibig JC. 2005. Bioassay analysis using R. *J Stat Softw* 12:1–22.
- Robert D, Malato S. 2002. Solar photocatalysis: A clean process for water detoxification. *Sci Total Environ* 291:85–97.
- Romero E, Schmitt P, Mansour M. 1994. Photolysis of pirimicarb in water under natural and simulated sunlight conditions. *Pestic Sci* 41:21–26.
- Rosenfeldt RR, Seitz F, Schulz R, Bundschuh M. 2014. Heavy metal uptake and toxicity in the presence of titaniumdioxide nanoparticles: A factorial approach using *Daphnia magna*. *Environ Sci Technol* 48:6965–6972.
- Ryan AC, Tomasso JR, Klaine SJ. 2009. Influence of pH, hardness, dissolved organic carbon concentration, and dissolved organic matter source on the acute toxicity of copper to *Daphnia magna* in soft waters: Implications for the biotic ligand model. *Environ Toxicol Chem* 28:1663–1670.
- Schwack W, Kopf G. 1993. Photodegradation of the carbamate insecticide pirimicarb. *Z Lebensm Unters Forsch* 197:264–268.
- Seitz F, Bundschuh M, Dabrunz A, Bandow N, Schaumann GE, Schulz R. 2012. Titanium dioxide nanoparticles detoxify pirimicarb under UV irradiation at ambient intensities. *Environ Toxicol Chem* 31:518–523.
- Seitz F, Lüderwald S, Rosenfeldt RR, Schulz R, Bundschuh M. 2015. Aging of TiO₂ nanoparticles transiently increases their toxicity to the pelagic microcrustacean *Daphnia magna*. *PLoS One* 10:e0126021.
- Seitz F, Rosenfeldt RR, Müller M, Lüderwald S, Schulz R, Bundschuh M. 2016. Quantity and quality of natural organic matter influence the ecotoxicity of titanium dioxide nanoparticles. *Nanotoxicology* 10:1415–1421.
- Sulzberger B, Durisch-Kaiser E. 2009. Chemical characterization of dissolved organic matter (DOM): A prerequisite for understanding UV-induced changes of DOM absorption properties and bioavailability. *Aquat Sci* 71:104–126.
- Thiruvengkatachari R, Vigneswaran S, Moon IS. 2008. A review on UV/TiO₂ photocatalytic oxidation process. *Korean J Chem Eng* 25:64–72.
- Turchi CS, Ollis DF. 1989. Mixed reactant photocatalysis: Intermediates and mutual rate inhibition. *J Catal* 119:483–496.
- US Environmental Protection Agency. 2006. Reregistration eligibility decision (RED) for permethrin. EPA 738-R-06-017. Washington, DC.
- Valenzuela MA, Bosch P, Jiménez-Becerrill J, Quiroz O, Páez AI. 2002. Preparation, characterization and photocatalytic activity of ZnO, Fe₂O₃ and ZnFe₂O₄. *J Photochem Photobiol A Chem* 148:177–182.
- Van Scoy A, Pennell A, Zhang X. 2016. Environmental fate and toxicology of dimethoate. *Rev Environ Contam Toxicol* 237:53–70.
- Westerhoff P, Song G, Hristovski K, Kiser MA. 2011. Occurrence and removal of titanium at full scale wastewater treatment plants: Implications for TiO₂ nanomaterials. *J Environ Monit* 13:1195–1203.
- Wheeler MW, Park RM, Bailer AJ. 2006. Comparing median lethal concentration values using confidence interval overlap or ratio tests. *Environ Toxicol Chem* 25:1441–1444.
- Xuereb B, Lefevre E, Garric J, Geffard O. 2009. Acetylcholinesterase activity in *Gammarus fossarum* (Crustacea Amphipoda): Linking AChE inhibition and behavioural alteration. *Aquat Toxicol* 94:114–122.
- Yang W, Gan J, Hunter W, Spurlock F. 2006. Effect of suspended solids on bioavailability of pyrethroid insecticides. *Environ Toxicol Chem* 25:1585–1591.
- Zoh KD, Kim TS, Kim JG, Choi K, Yi SM. 2006. Parathion degradation and toxicity reduction in solar photocatalysis and photolysis. *Water Sci Technol* 53:1–8.